Water Policy 21 (2019) 865–879

Management of the west-central Seto Inland Sea, Japan: factors controlling the spatiotemporal distributions of chlorophyll *a* concentration and Secchi depth

Feng Wang[a], Akira Umehara[b], Satoshi Nakai[a] and Wataru Nishijima[b,*]

[a]*Department of Chemical Engineering, Graduate School of Engineering, Hiroshima University, Hiroshima 739-8527, Japan*
[b]*Environmental Research and Management Center, Hiroshima University, Hiroshima 739-8513, Japan*
**Corresponding author. E-mail: wataru@hiroshima-u.ac.jp*

Abstract

Water quality data from 1981 to 2015 were used to elucidate the spatiotemporal distributions of chlorophyll *a* (Chl.*a*) concentration and Secchi depth in the west-central Seto Inland Sea, Japan. The results revealed that salinity and distance from the northern coastline were the main factors for predicting Chl.*a* concentration and Secchi depth, respectively. Significant differences in both of these were observed between subareas in spring, summer and autumn; differences were insignificant in winter. Chl.*a* concentrations have decreased for the past 35 years, while their extent differed in the subareas. A greater rate of decrease in Chl.*a* concentration was observed in the innermost Hiroshima Bay in spring, compared with other subareas, while no significant difference in different subareas was found in other seasons. Secchi depth has increased for the past 35 years, but no significant difference in its rate of increase was found among different subareas in all seasons. Total nitrogen loading better explained changes in mean Chl.*a* concentration than total phosphorus throughout the west-central Seto Inland Sea. Phytoplankton's contributions to light attenuation were low in the west-central Seto Inland Sea, indicating that the nutrient loading reduction programme has been of limited effectiveness in improving water clarity.

Keywords: Enclosed sea; Nutrient loading control; Phytoplankton; Secchi depth; West-central Seto Inland Sea

Introduction

In recent decades, anthropogenically increased nutrient loading has led to undesirable changes in ecosystem structures and functions, including overgrowth of phytoplankton in various coastal areas around the world (Orth *et al.*, 2006). Elevated chlorophyll *a* (*Chl.a*) concentrations decrease light intensity in

doi: 10.2166/wp.2019.177

the water column and can adversely impact the growth and production of seagrasses and benthic microalgae (Orth *et al*., 2006). Excess sedimentation and subsequent mineralization of dead phytoplankton cells in the sediment result in the production of reductive sediment and hypoxia of bottom waters, and marked changes in the benthos (Nishijima *et al*., 2015).

A variety of nutrient reduction programmes have been implemented following the deterioration in coastal waters through phytoplankton overgrowth, such as the Grizzle-Figg Act in relation to Tampa Bay, Florida, USA (Greening *et al*., 2014), the Action Plan for the Aquatic Environment in relation to Danish coastal waters (Riemann *et al*., 2016), a ban on phosphate-based detergents and the use of biological nitrogen removal in Chesapeake Bay, USA (Williams *et al*., 2010) and a Total Pollutant Load Control System (TPLCS) in Japanese enclosed waters including the Seto Inland Sea (Nakai *et al*., 2018; Nishijima *et al*., 2018). The results, however, have been dependent on the nature of pressures (e.g. type, magnitude, frequency and timing), connectivity with adjacent systems and differing water quality parameters (Carstensen *et al*., 2011; Duarte *et al*., 2015). In successful cases, the improvement appeared in nutrients, Chl.*a*, dissolved oxygen concentrations and seagrass cover after implementation of the programme (Greening *et al*., 2014; Riemann *et al*., 2016; Nakai *et al*., 2018; Nishijima *et al*., 2018), whereas little improvement or even worsening were unfortunately reported too (Williams *et al*., 2010; Riemann *et al*., 2016).

On the other hand, stable and appropriate primary production by phytoplankton, as well as by seagrasses and benthic microalgae, is essential to sustain the healthy functioning of ecosystems and the sustainable supply of fishery resources (Takai *et al*., 2002; Hoshika *et al*., 2006; Nakai *et al*., 2018). Phytoplankton growth will directly respond to nutrient supply, whereas the growth and distribution of benthic macro- and microalgae will be determined by both nutrient supply and light availability; the latter will also be affected by nutrient supply through phytoplankton growth. Therefore, nutrient loading reductions should be managed to maintain and improve both appropriate phytoplankton growth and light availability, and the responses of these water quality parameters to nutrient loading reductions need to be understood.

One effect of TPLCS implementation on the Seto Inland Sea has appeared in certain ecosystem components (Yamamoto, 2003; Nakai *et al*., 2018; Nishijima *et al*., 2018), although it varies in the subareas. The west-central Seto Inland Sea, including Hiroshima Bay and Aki Nada (Figure 1), receives substantial anthropogenic nutrient loading from its watersheds. Severe eutrophication in Hiroshima Bay (Seiki *et al*., 1991), especially the innermost region, is of great public concern because of its negative impact on ecosystem services. In addition, the west-central Seto Inland Sea is an archipelagic area, and the complex geographic conditions may significantly affect the characteristics of aquatic ecosystems, in which the responses to the reduction of the anthropogenic loadings may vary.

In this study, we constructed models estimating the spatiotemporal distributions of Chl.*a* concentration and Secchi depth in the west-central Seto Inland Sea and identified the definitive factors of these two water quality parameters in considering geographical characteristics such as salinity, water depth and distance from the coastline. Subsequently, based on the definitive factors, we classified the west-central Seto Inland Sea into different subareas. We then assessed the effect of the nutrient reduction programme on Chl.*a* concentrations and Secchi depth in each subarea of the west-central Seto Inland Sea to allow better environmental management. This study will not only enrich the literature showing responses to reduction of anthropogenic nutrient loadings in ecosystems but also help us gain a better understanding of the factors dominating standing phytoplankton stocks and light availability in such a semi-enclosed coastal ecosystem.

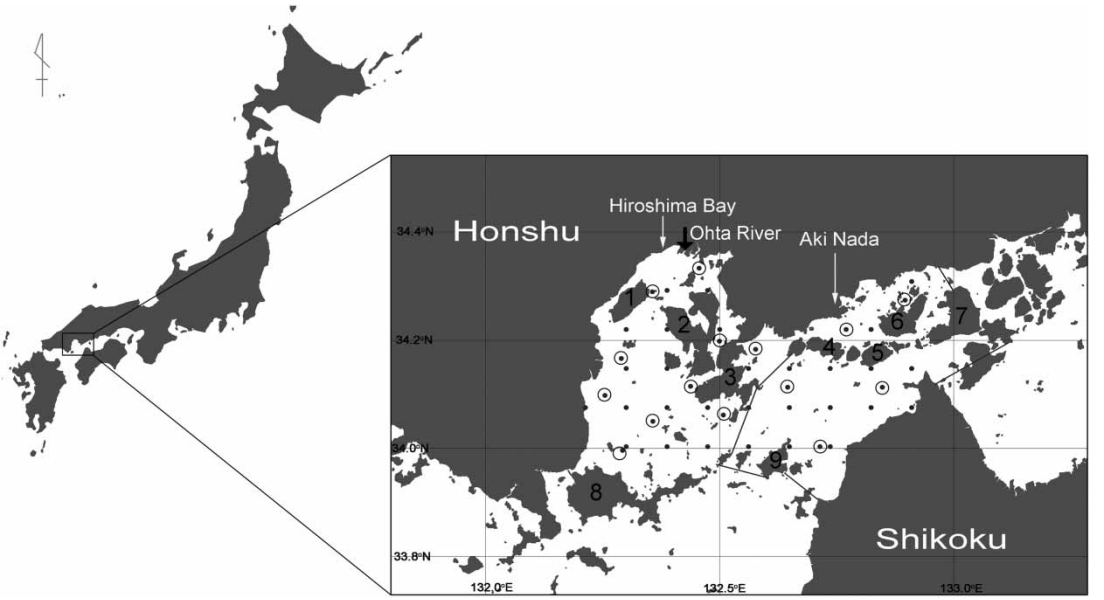

Fig. 1. Map of the west-central Seto Inland Sea. Dots in circles are monitoring sites from MOE and dots without circles are monitoring sites from MLIT. Numbers show Miyajima, Eta-Noumijima, Kurahashijima, Kamikamagarijima, Osakikamijima, Osakishimojima, Omishima, Yashirojima and Nakashima in order.

Methods

Study area

The west-central Seto Inland Sea consists of Hiroshima Bay (1,043 km^2) and Aki Nada (744 km^2) (Figure 1). Its southwestern part adjoins the Iyo Nada connected to the Pacific Ocean through the Bungo Channel. Bingo Nada and Hiuchi Nada connect to the east-central part of the Seto Inland Sea. Several large rivers over 20 km in length (e.g. Yahata, Ohta, Seno, Kurose, Nishiki and Noro Rivers) flow into the west-central Seto Inland Sea on its northern coastline (Honshu). There is no large river over 10 km in length flowing into the west-central Seto Inland Sea on its southern coastline (Shikoku). A chain of islands including Miyajima, Eta-Noumijima, Kurahashijima, Kamikamagarijima, Osakikamijima, Osakishimojima and Omishima are located within 5–10 km of the coast of Honshu. Another chain of islands including Yashirojima, Nakashima and some small islands constitute the southern border of the west-central Seto Inland Sea. Strong density stratification develops in warm seasons in the northwestern part of the area surrounded by the coast and the Miyajima and Eta-Noumijima islands. However, the waters in other parts mix well throughout the year (Asaoka *et al.*, 2018).

Data set

Seasonal water quality data (winter: mid-January to early February, spring: May, summer: July to early September, autumn: October) were provided by the Ministry of the Environment (MOE, 15 monitoring sites) for the period of 1981–2015. The Ministry of Land, Infrastructure, Transport and Tourism

(MLIT, 29 monitoring sites) provided information for the period of 2000–2014. Chl.*a* concentrations were not monitored for 13 of the 29 MLIT sites. Secchi depth, nutrient concentration, water temperature and water depth data were available for all 44 sites. The distance from the coastline of Honshu was derived by ArcGIS 10.2 (ESRI, 2011) for all monitoring sites.

The total nitrogen (TN) and total phosphorus (TP) loadings into the west-central Inland Sea were also provided by the MOE. Loadings have been estimated by the MOE as a part of the TPLCS every 5 years since 1979. The loading estimations took account of nutrient sources including industrial effluent, household discharges and agricultural wastewater.

Analysis

Secchi depth was twice measured with a 30-cm-diameter white disc by both the MLIT and the MOE, and the average of two records was used for data analysis. Water samples were taken at depths of 0.5 m and 2.0 m in the MOE and MLIT observations, respectively. Analyses of water temperature, salinity, nutrients (NH_4^+, NO_2^-, NO_3^-, TN, PO_4^{3-}, TP), and Chl.*a* were conducted in accordance with the Guidelines for Marine Observations (Japan Meteorological Agency, 2000).

*Factors influencing Chl.*a *concentration and Secchi depth*

The distance from the coastline and salinity is closely related with seston and nutrient levels in the water column since freshwater discharged from the land is a carrier of particles and nutrients. Water depth is an important indicator of resuspension of sediment particles, which play important roles in the variations in light conditions or Chl.*a* concentrations in the water column. The effect of distance from the island coastlines and that from those of the southern margins (Shikoku), however, are much less important than that from the coastline of Honshu (the northern coastline). This is because there are no (or only small) rivers, and no significant point sources of nutrients, in the islands and the southern area of land (Figure S1, available with the online version of this paper). Therefore, we chose the distance from the nearest northern coastline as a geographical parameter. The Spearman rank correlation coefficients were used to determine the degree of correlation between distance, salinity, water depth, water temperature, Chl.*a* concentration and Secchi depth.

A logistic curve or logistic growth curve had been successfully used for predicting continuous variables with thresholds (e.g. Zwietering *et al.*, 1990; Kucharavy & De Guio, 2015). Equation (1) (Figure S2 as an example, available online) and Equation (2) based on Zwietering *et al.* (1990) and Hara (1999) were used to predict Secchi depth or Chl.*a* concentration with distance from the northern coastline, water depth and surface salinity (hereafter referred to as distance from the coastline, depth and salinity, respectively) using the 'lsqcurvefit' function (https://ww2.mathworks.cn/help/optim/ug/lsqcurvefit.html) of MATLAB R2014b (MathWorks, Inc., Natick, Massachusetts, USA):

$$A = 1/(b_1 + b_2 \times \exp(b_3 \times x)) \tag{1}$$

$$A = 1/(b_1 + b_2 \times \exp(b_3 \times x_1 + b_4 \times x_2)) \tag{2}$$

where A was SD or Chl.*a*, and x was normalized distance, salinity or depth (z-score normalization based on mean and standard deviation). x_1 and x_2 were two factors from normalized distance, salinity and depth. b_1, b_2, b_3 and b_4 were coefficients. Equation (1) was used to find the best determinant factor

to predict Secchi depth or Chl.*a* concentration. Equation (2) was used to find the best combination of factors to predict these two.

The best combination of distance from the coastline, salinity and depth derived from the above equations was then used to classify the 31 monitoring sites with Chl.*a* concentration data into classes based on the results of agglomerative hierarchical clustering. The agglomerative hierarchical clustering of Euclidean distance was conducted with an average linkage criteria method using R software (R Core Team, 2015). The distance from the northern coastline and salinity (results from later analysis) were used after square-root-transformed and normalized for the clustering analysis. Then, the monitoring sites were classified using the dendrogram obtained by the clustering.

Estimation of phytoplankton contribution to light attenuation

Nishijima *et al.* (2018) separate the roles of non-phytoplankton components from total optical active components contributing to light attenuation and propose a novel indicator background Secchi depth (BSD). BSD applies when the influence of phytoplankton is absent; that is, when Chl.*a* concentration equals 0. We estimated phytoplankton contribution to light attenuation, based on the concept of BSD, as follows (Equations (3)–(9)):

$$K_{\mathrm{d}} = K_{\mathrm{W}} + K_{\mathrm{CDOM}} + K_{\mathrm{tripton}} + K_{\mathrm{phyt}} \tag{3}$$

$$K_{\mathrm{bg}} = K_{\mathrm{W}} + K_{\mathrm{CDOM}} + K_{\mathrm{tripton}} \tag{4}$$

$$K_{\mathrm{d}} = K_{\mathrm{bg}} + K_{\mathrm{phyt}} \tag{5}$$

$$K_{\mathrm{d}} = a/\mathrm{SD} \tag{6}$$

$$K_{\mathrm{bg}} = a/\mathrm{BSD} \tag{7}$$

$$\mathrm{phyt}\% = 100 \times (1 - K_{\mathrm{bg}}/K_{\mathrm{d}}) \tag{8}$$

$$\mathrm{phyt}\% = 100 \times (1 - \mathrm{SD}/\mathrm{BSD}) \tag{9}$$

In Equation (3), K_{d} is the total light attenuation coefficient for the water column, and K_{w}, K_{CDOM}, K_{tripton} and K_{phyt} are partial light attenuation by water, chromophoric dissolved organic matters (CDOM), tripton and phytoplankton, respectively. In Equation (4), K_{bg} is the attenuation caused by background factors, which is the sum of K_{w}, K_{CDOM} and K_{tripton} in Equation (3) (Nishijima *et al.*, 2018). In Equations (6) and (7), SD is Secchi depth and BSD is the background Secchi depth. The coefficient a is the product of K_{d} and SD or the product of K_{bg} and BSD. In Equations (8) and (9), phyt% is phytoplankton contribution in light attenuation. The average phyt% at a monitoring site is then obtained from Equation (9) when average SD is used.

Statistical analysis

Harmonic and arithmetic means were used for Secchi depth and other water quality parameters, respectively. Standard deviation in the harmonic mean was calculated based on the method reported by Lam *et al.* (1985). Kruskal–Wallis analysis of variance (ANOVA) tests and subsequent Dunn's

tests for multiple comparisons were used to compare Chl.*a* concentration and Secchi depth in different subareas. Bonferroni corrections were used for multiple comparisons. Chl.*a* and Secchi depth data from the MOE during the period 1981–2015 were analysed for monotonously increasing or decreasing trends with linear regression. Influencers of the linear regression model were identified and removed by DFFITS (difference in fits, Belsley *et al*., 1980). Tukey's HSD test was used for multiple comparisons of regression slopes of linear models in different seasons of each subarea of the west-central Seto Inland Sea. The Kruskal–Wallis test, Dunn's test and Tukey's HSD test were performed with R software (R Core Team, 2015). A value of $p < 0.05$ was considered to be statistically significant in these tests.

Results and discussion

*Spatial distribution of Secchi depth and Chl.*a *concentration, 2000–2014*

Water temperatures in the west-central Seto Inland Sea showed a typical seasonal variability. The mean water temperatures at the 44 monitoring sites were 10.2–12.6 °C (winter), 15.3–18.8 °C (spring), 22.1–26.2 °C (summer) and 22.3–23.7 °C (autumn). Salinity was the lowest in summer (22.7–32.9) and the highest in winter (31.2–33.6). Chl.*a* concentration at the surface of the west-central Seto Inland Sea varied greatly by seasons and locations (Figure S3, available with the online version of this paper). The values peaked in summer (1.1–14.5 $\mu g\ l^{-1}$), declined in autumn (1.0–8.7 $\mu g\ l^{-1}$) and winter (0.8–3.5 $\mu g\ l^{-1}$), and rose in spring (0.6–6.9 $\mu g\ l^{-1}$). Secchi depth in the west-central Seto Inland Sea ranged from 2.0 to 8.4 m (Figure S4, available online), with higher values observed in winter (4.0–8.4 m) and lower values in summer (2.1–7.6 m).

The Spearman correlation coefficients between Chl.*a*, Secchi depth and other geographical and water quality parameters, including distance from the northern coastline, salinity, water depth, dissolved inorganic nitrogen (DIN) and dissolved inorganic phosphorus (DIP), in different seasons during the period 2000–2014 are summarized in Table 1. The Chl.*a* concentrations were best related to salinity (r: –0.89 to –0.48, $p < 0.01$) and the distance from the northern coastline (r: 0.45–0.80, $p < 0.05$), while Secchi depth was best related to the distance from the northern coastline (r: 0.36–0.82, $p < 0.05$) and depth (r: 0.37–0.56, $p < 0.05$). Secchi depth was also significantly correlated with salinity, except for winter when the variation of salinity was smaller than that in other seasons due to smaller river flow into the study area. Significant correlations were also found between Chl.*a* concentration and Secchi

Table 1. Spearman correlation coefficients for the relationship among distance, depth, salinity, water temperature, chlorophyll *a* (Chl.*a*) and Secchi depth, 2000–2014.

Item	Season	Distance	Depth	Salinity	Temp.	DIN	DIP	Chl.*a*
Chl.*a*	Spring	−0.57**	−0.45*	−0.82**	0.80*	0.41*	−0.50*	
	Summer	−0.45*	−0.20	−0.48**	0.45**	0.16	−0.15	
	Autumn	−0.80**	−0.52*	−0.89**	−0.03	0.01	0.02	
	Winter	−0.61**	−0.60*	−0.55**	−0.45**	−0.42*	−0.50*	
Secchi	Spring	0.82**	0.56*	0.57**	−0.56*	−0.25	0.11	−0.68**
	Summer	0.78**	0.38*	0.40*	−0.23	−0.34	0.03	−0.66**
	Autumn	0.79**	0.37*	0.65**	−0.01	−0.19	0.07	−0.66**
	Winter	0.36*	0.41*	0.13	0.06	−0.08	−0.21	0.01

Note: Temp. is water temperature; *$p < 0.05$; **$p < 0.01$.

depth in spring, summer and autumn (r: 0.66–0.68, $p < 0.01$). Although DIN and DIP are the important factors in the control of Chl.*a* concentration, they did not show a positive relationship with Chl.*a* concentration except for spring (r: 0.41, $p < 0.05$).

*Factors determining Chl.*a *concentration and Secchi depth*

We tried to find factors determining the Chl.*a* concentration and Secchi depth in the west-central Seto Inland Sea. The results of logistic curve fitting are shown in Tables 2 and 3 and Tables S1 and S2 (available online). Salinity was the best individual predictor of Chl.*a* concentrations, especially from spring to autumn (R^2: 0.81–0.90). The supply of nutrients through freshwater will contribute to phytoplankton growth, but nutrients were also supplied from adjacent waters connecting to the study waters. The contribution of the Pacific Ocean to TN and TP loadings into the study area was estimated to be about 80%–90% and about 75%, respectively (Ishii & Yanagi, 2004). Therefore, the significant relationship between Chl.*a* concentration and salinity would not mean simply that Chl.*a* concentration was controlled by nutrients from the land. Low salinity areas are mainly located on shallow coasts, suggesting that salinity represents not only the nutrient supply from the land but also the various effects of the land.

The distance was the best individual predictor of Secchi depth in the study area (Table 3, R^2: 0.58–0.74) in spring, summer and autumn, whereas salinity showed low correlation with Secchi depth (Table 3, R^2: 0.02–0.43). Moreover, depth was weakly correlated with Secchi depth even though the Chl.*a* concentration was not related to depth. Hibino & Matsumoto (2006) reported that the sediment

Table 2. Performance of logistic curve fitting to predict chlorophyll *a* with different combinations of distance from the coast, water depth and salinity.

	Spring		Summer		Autumn		Winter	
Predictors	R^2	RMSE	R^2	RMSE	R^2	RMSE	R^2	RMSE
Distance	0.26	1.27	0.24	2.44	0.41	1.44	0.44	0.62
Depth	0.04	1.45	0.01	2.77	0.09	1.79	0.34	0.67
Salinity	0.90	0.46	0.94	0.68	0.81	0.82	0.45	0.61
Distance + depth	0.26	1.29	0.24	2.48	0.41	1.47	0.48	0.60
Distance + salinity	0.91	0.46	0.95	0.65	0.86	0.72	0.49	0.60
Depth + salinity	0.91	0.46	0.94	0.67	0.83	0.80	0.48	0.60

Table 3. Performance of logistic curve fitting to predict Secchi depth with different combinations of distance from the coast, water depth and salinity.

	Spring		Summer		Autumn		Winter	
Predictors	R^2	RMSE	R^2	RMSE	R^2	RMSE	R^2	RMSE
Distance	0.74	0.65	0.58	0.85	0.65	0.71	0.20	1.11
Depth	0.20	1.16	0.11	1.23	0.17	1.09	0.11	1.16
Salinity	0.38	1.02	0.43	0.98	0.30	1.00	0.02	1.22
Distance + depth	0.75	0.65	0.58	0.86	0.65	0.72	0.23	1.09
Distance + salinity	0.75	0.65	0.68	0.75	0.66	0.70	0.45	0.93
Depth + salinity	0.43	0.99	0.49	0.94	0.39	0.94	0.10	1.18

was covered with 1–6 cm of thin floating mud in the wide area of the northern part of Hiroshima Bay. In addition, suspended solids in the waterbody were supplied from floating mud on the sediment near the coastline and transported southward (Lee *et al*., 2001). This might be the reason for the good correlation between the distance from the northern coastline and Secchi depth.

Since the combinational use of distance from the northern coastline and salinity in the logistic curves successfully predicted the Chl.*a* concentration and Secchi depth, these were used to explore the mechanisms underpinning the Chl.*a* and Secchi depth distribution regime in the west-central Seto Inland Sea. The whole west-central Seto Inland Sea was divided into three classes by the agglomerative hierarchical clustering method (Figure 2). The monitoring sites belonging to Class 1, characterized by low salinity and a short distance from coastline, were located in the innermost part of Hiroshima Bay. The monitoring sites in Class 2, with median salinity and at a short distance from the coastline, were distributed in western coastal Hiroshima Bay and northern coastal Aki Nada. The monitoring sites in Class 3 were distributed in the area far away from the northern coastline.

*Spatial and historical changes in Chl.*a *concentration and Secchi depth in the west-central Seto Inland Sea*

The seasonal mean Chl.*a* concentration and Secchi depth during the period 2000–2014 in the classified subareas of the west-central Seto Inland Sea are shown in Figure 3. A significant difference among the subareas of the west-central Seto Inland Sea was observed in spring, summer and autumn for both Chl.*a* and Secchi depth ($p < 0.05$); no significant differences were observed in winter ($p > 0.05$). Generally, subarea Class 1 showed the highest Chl.*a* concentration, followed by Class 2 and Class 3 during spring, summer and autumn. By contrast, the highest Secchi depth was observed in subarea Class 3, followed by Class 2 and Class 1 in spring, summer and autumn. In winter, the large water mixing by the strong wind and the sea surface cooling could be responsible for the small regional difference in Chl.*a* and Secchi depth.

The annual values in Chl.*a* and Secchi depth in different subareas of the west-central Seto Inland Sea during the past 35 years (1981–2015) are shown in Figures 4 and 5. Significant decreases in mean Chl.*a* concentration were observed during a specific season in the coastal regions (Classes 1 and 2) and during several seasons in the offshore region (Class 3). In spring, the decreasing rate of mean Chl.*a* concentration expressed as a slope factor in Class 1 (0.177 $\mu g\, l^{-1}\, year^{-1}$) was significantly higher than those in Classes 2 and 3 (0.024–0.025 $\mu g\, l^{-1}\, year^{-1}$, $p < 0.05$). Although large fluctuations in mean Chl.*a* concentration were observed, the rates of decrease were also higher during summer (0.154 $\mu g\, l^{-1}\, year^{-1}$) and autumn (0.100 $\mu g\, l^{-1}\, year^{-1}$) in Class 1 than those in Classes 2 and 3.

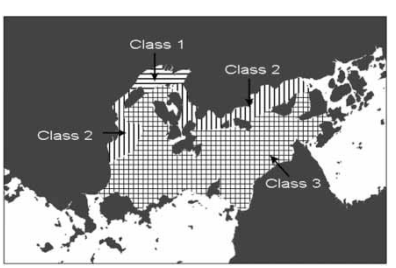

Fig. 2. Classification of the west-central Seto Inland Sea based on distance from the northern coastline and salinity.

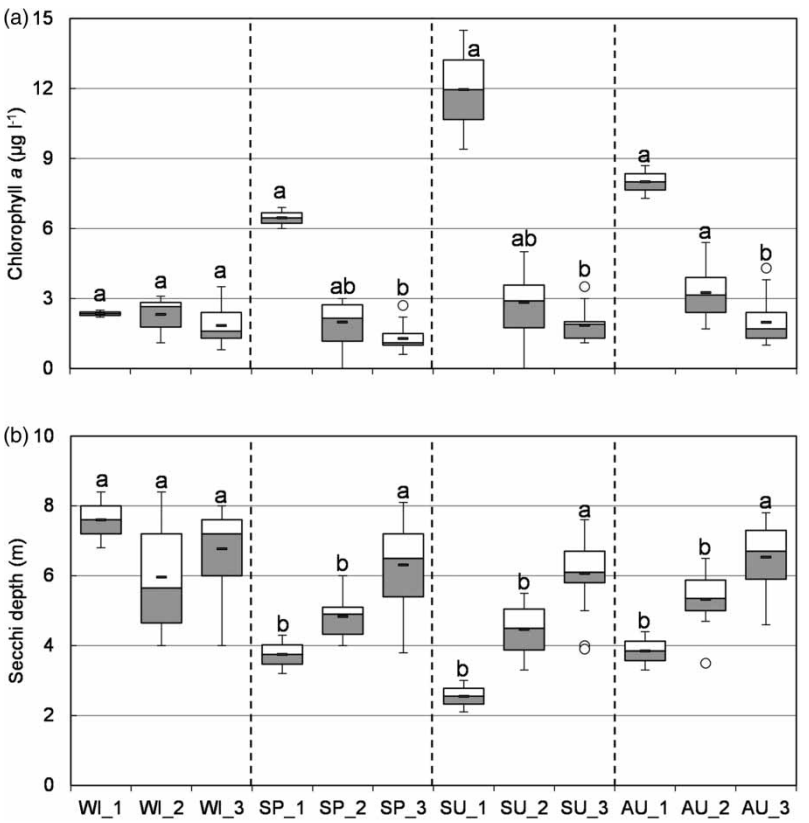

Fig. 3. Seasonal mean chlorophyll *a* concentration (a) and the mean Secchi depth (b) in different subareas of the west-central Seto Inland Sea. WI, SP, SU and AU = winter, spring, summer and autumn, respectively. 1, 2 and 3 = Class 1, Class 2 and Class 3, respectively (see Figure 2). 'o' = the outlier by 1.5 interquartile range (IQR) rule. Within each season, boxes with different letters (a, b) indicate significant differences ($p < 0.05$, Dunn's test) between different subareas.

Secchi depth was observed to increase with time in most cases. A significant increase ($p < 0.05$) in the mean Secchi depth was observed during several seasons in the regions of Classes 2 and 3 (Figure 5). No significant difference was found in the rate of increase in the mean Secchi depth among Classes 1–3 in all seasons, because of high fluctuation and low rates of increase. Moreover, Secchi depth is determined not only by phytoplankton concentration but also by other factors which will not change by eutrophication.

Chl.*a* concentration has decreased in the west-central Seto Inland Sea, although the extent of reduction has varied both seasonally and spatially. This may be a positive response to the implementation of TPLCS in this area. During the 30 years from 1979 to 2009, the TP and TN entering the west-central Seto Inland Sea from the land declined by 45.45% and 25.76%, respectively (Table 4). The mean Chl.*a* concentration in each classified area for 5-year intervals was plotted against TN and TP loadings from the land during the corresponding time intervals to check the relationship between allochthonous nutrient loading and phytoplankton abundance (Figure S5, available online). For example, the mean Chl.*a* concentration from 1981 to 1985 was paired with the nutrient loading in 1984. Class 1 was located in Hiroshima Bay, and Class 2 was mainly located in Hiroshima Bay, so the mean Chl.*a* concentrations were paired with nutrient loads in

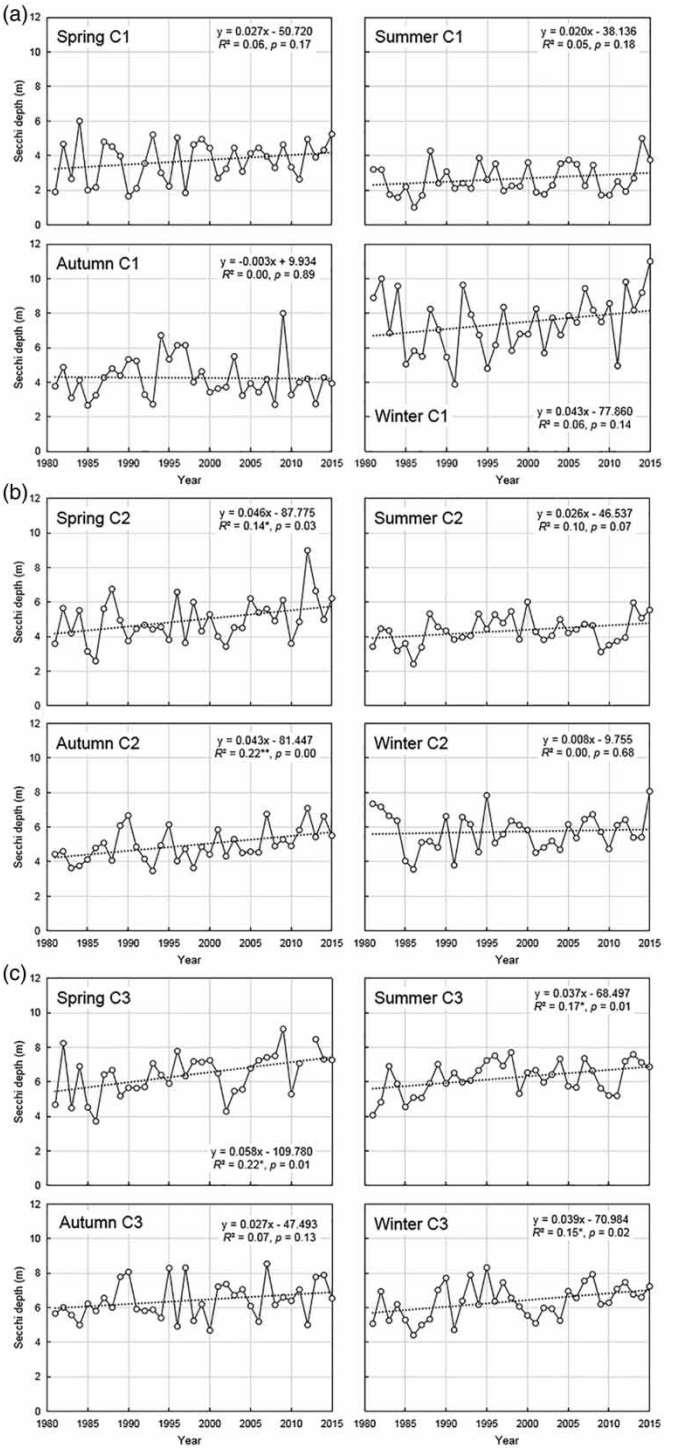

Fig. 4. Time course of mean chlorophyll *a* concentration in different subareas of west-central Seto Inland Sea, 1981–2015. C1 (a), C2 (b), C3 (c) = Classes 1, 2 and 3, respectively (see Figure 2). *Note*: $*p < 0.05$; $**p < 0.01$.

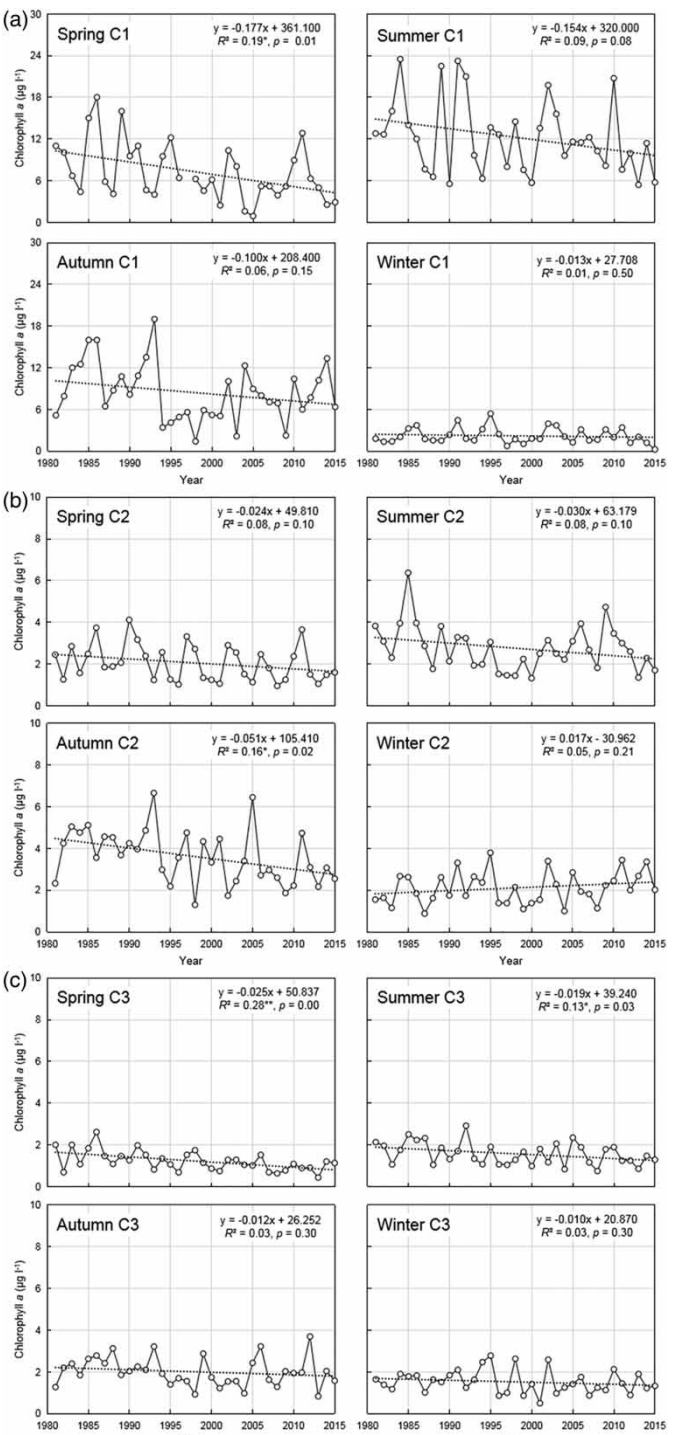

Fig. 5. Time course of the mean Secchi depth in different subareas of west-central Seto Inland Sea, 1981–2015. C1 (a), C2 (b), C3 (c) = Classes 1, 2 and 3, respectively (see Figure 2). *Note*: $*p < 0.05$; $**p < 0.01$.

Table 4. Nutrient loading (kg km^{-2} day^{-1}) from the surrounding land into the west-central Seto Inland Sea.

Area	Loading	Year							Decrease (%)[a]
		1979	1984	1989	1994	1999	2004	2009	
Hiroshima Bay	TN	31.6	30.7	32.6	28.7	25.9	24.0	22.6	28.71
	TP	2.97	2.01	2.30	2.43	2.30	1.53	1.55	47.96
Aki Nada	TN	10.8	9.4	9.4	10.2	9.4	9.4	9.2	14.48
	TP	1.08	0.81	0.81	0.79	0.81	0.67	0.66	38.34
Average	TN	22.9	21.8	22.9	21.0	19.0	17.9	17.0	25.76
	TP	2.18	1.51	1.68	1.75	1.68	1.18	1.18	45.45

[a]Decrease (%) $= 100 \times (\mathrm{Load}_{1979} - \mathrm{Load}_{2009})/\mathrm{Load}_{1979}$.

Hiroshima Bay for Classes 1 and 2. The mean Chl.*a* concentrations were paired with average nutrient loads in Hiroshima Bay and Aki Nada for Class 3. The results suggested that Chl.*a* may be impacted by the TN loading (R^2: 0.46–0.62) greater than TP loading (R^2: 0.05–0.21) throughout the west-central Seto Inland Sea. Although the decrease in Chl.*a* concentration with the decrease in nutrient loading from the land was observed to be clearer in Classes 1 and 2 (facing the large sources of nutrients from rivers) than in Class 3, statistical significance was not observed in either case. Our result is consistent with a nutrient enrichment algal assay conducted by Lee *et al.* (1996), which reported that the growth of the entire phytoplankton community in Hiroshima Bay was stimulated by the addition of nitrogen.

In the west-central Seto Inland Sea, the molar ratios of DIN to DIP showed extremely high variations. It was lower than the Redfield ratio of 16 with some exceptions in the subareas of Classes 2 and 3 and around 30 in the subarea of Class 1 (Table S3, available online). Nutrient release from the sediment and nutrient supply from the connecting waters should be considered as other sources. In nutrient release from the sediment, greater amounts of phosphorus than nitrogen are known to be released and to enter the overlying waters, especially in the warmer seasons (Lee & Hoshika, 2000). In the nutrient supply from the connecting waters, DIN:DIP ratios in Iyo Nada, Bingo Nada and Hiuchi Nada were less than or around 16 in most cases. Consequently, the result that the Chl.*a* concentration showed a better correlation with TN loading than with TP loading would be reasonable. Dissolved silicate is also an important nutrient for phytoplankton growth. In an investigation across the Seto Inland Sea, it was proved not to be a limiting nutrient, except in Osaka Bay during the period 1994–2000 (Yanagi & Harashima, 2003).

On the other hand, phosphorus is reported to control Chl.*a* concentration in Suo Nada, west of this study area in the Seto Inland Sea (Nishijima *et al.*, 2016). The main differences between the water in this study, Hiroshima Bay and Aki Nada, and Suo Nada, were DIN:DIP ratios in the water column and nutrient loadings from the land. The DIN:DIP ratios in the water column ranged from 17.0 to 35.2 in the shallow area (less than 20 m). Those in nutrient loadings from the land ranged from 17.7 to 19.0 after 1989 in Suo Nada. On the other hand, the DIN:DIP ratios in the water column ranged from 6.3 to 16.4, with one exception: the deep area connected to Iyo Nada. These results suggested that the shallow area near the coastline was strongly affected by nutrient loadings from the land, and a higher ratio (>16) of DIN:DIP in nutrient loading from land resulted in phosphorus limiting phytoplankton growth in Suo Nada. Not only the amount of nutrients supplied from the land but also the ratio of DIN:DIP was found to control phytoplankton growth, especially in coastal areas.

Secchi depth in the west-central Seto Inland Sea has also improved over the past 35 years, but rates of increase were small (less than 0.05 m $year^{-1}$) and accompanied with large annual fluctuations.

Table 5. Phytoplankton contribution to light attenuation in the classified areas of the west-central Seto Inland Sea.

Season	Class 1	Class 2	Class 3
Spring	28.3%	22.1%	19.9%
Summer	35.2%	21.1%	12.6%
Autumn	28.4%	15.1%	14.6%
Winter	26.6%	10.3%	4.5%

Secchi depth is influenced by multiple optical factors affecting light attenuation in the water column, including phytoplankton and other background factors such as sea water, tripton and CDOM (Christian & Sheng, 2003; Devlin *et al*., 2008). In most parts of the west-central Seto Inland Sea, phytoplankton contribution to light attenuation was surprisingly limited, being less than 36% in Class 1 and less than 23% in Classes 2 and 3 (Table 5). Phytoplankton contribution to light attenuation in Classes 2 and 3 in the west-central Seto Inland Sea was less than that reported in Harima Nada, the Seto Inland Sea (27%, Yamaguchi *et al*., 2013). Being more archipelagic than Harima Nada, the west-central Seto Inland Sea could support higher tripton levels in the offshore area, resulting in lower phytoplankton contribution to light attenuation. The reduction in Chl.*a* concentration in these areas was also modest, implying that the improvement in Secchi depth through a decrease in Chl.*a* concentration via TPLCS may be limited in the west-central Seto Inland Sea.

Implications for future policy-making and management

The management of Seto Inland Sea has undergone a major and positive shift from water quality control to environmental remediation and restoration of habitat in the revision of Act on Special Measures concerning the Conservation of the Environment of the Seto Inland Sea in 2015, which aimed at realizing a beautiful and bountiful sea (Nakai *et al*., 2018). Under the new management framework, restoration of seagrass and seaweed beds constituted an important part, which would rely much on the improvement of water clarity. This article emphasized the role of natural environmental conditions, e.g. salinity or suspended solids in water as crucial for water quality, especially the water clarity. Considering the phytoplankton's low contribution to light attenuation in the west-central Seto Inland Sea, the improvement of water clarity via the TPLCS by decreasing phytoplankton concentration would be limited. Without our achievement, policy-makers and environmental managers in the Seto Inland Sea may depend too much on water quality improvement through the TPLCS in seaweed and seagrass restoration. We should tackle not only the natural increase of seaweed and seagrass by the improvement of water quality but also seaweed and seagrass bed construction by raising a bottom to improve the light condition. These findings in the west-central Seto Inland Sea are expected to apply in other semi-enclosed waters receiving both substantial freshwater input and anthropogenic nutrient loads. Moreover, due to the highly variable natural condition in these regions, decadal time frames or flexible agenda should be used to allow significant or detectable improvements in coastal water quality.

Conclusions

This study identified salinity and distance from the northern coastline to be the most definitive factors for Chl.*a* concentration and Secchi depth in the west-central Seto Inland Sea, respectively, based on

monitoring records for the period of 2006–2015. Significant differences were observed among the subareas of the west-central Seto Inland Sea during spring, summer and autumn in both Chl.*a* concentration and Secchi depth, while no significant difference existed in winter. The large water mixing by the strong wind and the sea surface cooling during winter could be responsible for the small regional difference in Chl.*a* concentration and Secchi depth.

The application of the TPLCS to the watershed of the west-central Seto Inland Sea since 1979 has resulted in a 45.45% reduction in TP loading and 25.76% reduction in TN loading from 1979 to 2009. The Chl.*a* concentration has decreased, although the extent of reduction varies both seasonally and spatially. In the innermost Hiroshima Bay (Class 1), the mean Chl.*a* concentration underwent a significantly higher rate of decrease than other subareas of the west-central Seto Inland Sea during the spring of the past 35 years, while no significant difference in the rate of decrease among the subareas was found in other seasons. Secchi depth in the west-central Seto Inland Sea also showed a trend of improvement over the past 35 years. However, the difference in increasing rates of the mean Secchi depth among the subareas was insignificant in all seasons. Finally, considering the phytoplankton's low contribution to light attenuation in the west-central Seto Inland Sea, the influence of TPLCS on improvement in water clarity via decreasing phytoplankton concentration was limited.

Acknowledgements

Special thanks are given to the Ministry of the Environment and the Ministry of Land, Infrastructure, Transport and Tourism, Japan, for supplying data from their investigation of the Seto Inland Sea. We are grateful to Environmental Consultants for Ocean and Human Corporation for providing the nutrient loading data. This study was supported by a grant from the Environment Research and Technology Development Fund (S-13) of the Ministry of the Environment, Japan (S-13).

References

Asaoka, S., Umehara, A., Otani, S., Fujii, N., Okuda, T., Nakai, S., Nishijima, W., Takeuchi, K., Shibata, H. & Jadoon, W. A. (2018). Spatial distribution of hydrogen sulfide and sulfur species in coastal marine sediments Hiroshima Bay, Japan. *Marine Pollution Bulletin 133*, 891–899.

Belsley, D., Kuh, E. & Welsh, R. (1980). *Regression Diagnostics: Identifying Influential Data and Sources of Collinearity. Wiley Series in Probability and Mathematical Statistics*. John Wiley & Sons, New York, pp. 11–16.

Carstensen, J., Sánchez-Camacho, M., Duarte, C. M., Krause-Jensen, D. & Marba, N. (2011). Connecting the dots: responses of coastal ecosystems to changing nutrient concentrations. *Environmental Science & Technology 45*, 9122–9132.

Christian, D. & Sheng, Y. P. (2003). Relative influence of various water quality parameters on light attenuation in Indian River Lagoon. *Estuarine, Coastal and Shelf Science 57*, 961–971.

Devlin, M., Barry, J., Mills, D., Gowen, R., Foden, J., Sivyer, D. & Tett, P. (2008). Relationships between suspended particulate material, light attenuation and Secchi depth in UK marine waters. *Estuarine, Coastal and Shelf Science 79*, 429–439.

Duarte, C. M., Borja, A., Carstensen, J., Elliott, M., Krause-Jensen, D. & Marbà, N. (2015). Paradigms in the recovery of estuarine and coastal ecosystems. *Estuaries and Coasts 38*, 1202–1212.

ESRI (2011). *ArcGIS Desktop: Release 10*. Environmental Systems Research Institute, Redlands, CA.

Greening, H., Janicki, A., Sherwood, E. T., Pribble, R. & Johansson, J. O. R. (2014). Ecosystem responses to long-term nutrient management in an urban estuary: Tampa Bay, Florida, USA. *Estuarine, Coastal and Shelf Science 151*, A1–A16.

Hara, Y. (1999). Calculation of population parameters using Richards function and application of indices of growth and seed vigor to rice plants. *Plant Production Science 2*(2), 129–135.

Hibino, T. & Matsumoto, H. (2006). Distribution of fluid mud layer in Hiroshima Bay and its seasonal variation. *Journal of JSCE B 62*, 348–359.

Hoshika, A., Sarker, M. J., Ishida, S., Mishima, Y. & Takai, N. (2006). Food web analysis of an eelgrass (*Zostera marina* L.) meadow and neighbouring sites in Mitsukuchi Bay (Seto Inland Sea, Japan) using carbon and nitrogen stable isotope ratios. *Aquatic Botany 85*, 191–197.

Ishii, D. & Yanagi, T. (2004). Origins and variable mechanisms of total phosphorus and total nitrogen concentrations in the Seto Inland Sea. *Oceanography in Japan 13*, 389–401 (in Japanese).

Japan Meteorological Agency (2000). *Guidelines for Marine Observations*. The Oceanographic Society of Japan, Tokyo.

Kucharavy, D. & De Guio, R. (2015). Application of logistic growth curve. *Procedia Engineering 131*, 280–290.

Lam, F. C., Hung, C. T. & Perrier, D. G. (1985). Estimation of variance for harmonic mean half-lives. *Journal of Pharmaceutical Sciences 74*(1), 229–231.

Lee, I. & Hoshika, A. (2000). Seasonal variations in pollutant loads and water quality in Hiroshima Bay. *Journal of Water Environment Society 23*, 367–373 (in Japanese with English abstract).

Lee, Y. S., Seiki, T., Mukai, T., Takimoto, K. & Okada, M. (1996). Limiting nutrients of phytoplankton community in Hiroshima Bay, Japan. *Water Research 30*, 1490–1494.

Lee, I., Fujita, K., Takasugi, Y. & Hoshika, A. (2001). Numerical simulation of residual current and material transportation in Hiroshima Bay. *Oceanography in Japan 10*(6), 495–507 (in Japanese with English abstract).

Nakai, S., Soga, Y., Sekito, S., Umehara, A., Okuda, T., Ohno, M., Nishijima, W. & Asaoka, S. (2018). Historical changes in primary production in the Seto Inland Sea, Japan, after implementing regulations to control the pollutant loads. *Water Policy 20*(4), 855–870.

Nishijima, W., Umehara, A., Okuda, T. & Nakai, S. (2015). Variations in macrobenthic community structures in relation to environmental variables in the Seto Inland Sea, Japan. *Marine Pollution Bulletin 92*, 90–98.

Nishijima, W., Umehara, A., Sekito, S., Okuda, T. & Nakai, S. (2016). Spatial and temporal distributions of Secchi depths and chlorophyll *a* concentrations in the Suo Nada of the Seto Inland Sea, Japan, exposed to anthropogenic nutrient loading. *Science of The Total Environment 571*, 543–550.

Nishijima, W., Umehara, A., Sekito, S., Wang, F., Okuda, T. & Nakai, S. (2018). Determination and distribution of region-specific background Secchi depth based on long-term monitoring data in the Seto Inland Sea, Japan. *Ecological Indicators 84*, 583–589.

Orth, R. J., Carruthers, T. J., Dennison, W. C., Duarte, C. M., Fourqurean, J. W., Heck, K. L., Hughes, A. R., Kendrick, G. A., Kenworthy, W. J. & Olyarnik, S. (2006). A global crisis for seagrass ecosystems. *AIBS Bulletin 56*, 987–996.

R Core Team (2015). *R: A Language and Environment for Statistical Computing*. Vienna, Austria.

Riemann, B., Carstensen, J., Dahl, K., Fossing, H., Hansen, J. W., Jakobsen, H. H., Josefson, A. B., Krause-Jensen, D., Markager, S. & Stæhr, P. A. (2016). Recovery of Danish coastal ecosystems after reductions in nutrient loading: a holistic ecosystem approach. *Estuaries and Coasts 39*, 82–97.

Seiki, T., Date, E. & Izawa, H. (1991). Eutrophication in Hiroshima Bay. *Marine Pollution Bulletin 23*, 95–99.

Takai, N., Mishima, Y., Yorozu, A. & Hoshika, A. (2002). Carbon sources for demersal fish in the western Seto Inland Sea, Japan, examined by δ13c and δ15n analyses. *Limnology and Oceanography 47*, 730–741.

Williams, M. R., Filoso, S., Longstaff, B. J. & Dennison, W. C. (2010). Long-term trends of water quality and biotic metrics in Chesapeake Bay: 1986 to 2008. *Estuaries and Coasts 33*, 1279–1299.

Yamaguchi, H., Katahira, R., Ichimi, K. & Tada, K. (2013). Optically active components and light attenuation in an offshore station of Harima Sound, eastern Seto Inland Sea, Japan. *Hydrobiologia 714*(1), 49–59.

Yamamoto, T. (2003). The Seto Inland Sea – eutrophic or oligotrophic? *Marine Pollution Bulletin 47*, 37–42.

Yanagi, T. & Harashima, A. (2003). Characteristics of dissolved inorganic phosphorus, nitrogen and silicate distributions in the Seto Inland Sea. *Oceanography in Japan 12*, 565–572 (in Japanese with English abstract).

Zwietering, M. H., Jongenburger, I., Rombouts, F. M. & Van't Riet, K. (1990). Modeling of the bacterial growth curve. *Applied and Environmental Microbiology 56*(6), 1875–1881.

Received 16 August 2018; accepted in revised form 3 April 2019. Available online 6 May 2019